

MOVING HEATERS AS A MODEL OF CONTINENTAL DRIFT*

J. A. WHITEHEAD

*Institute of Geophysics and Planetary Physics, University of California, Los Angeles, Los Angeles, Calif. 90024, U.S.A.***

Received April 1971

The dynamical behavior of vertical and horizontal movements of floating heat sources is studied experimentally and theoretically. The study of the properties of horizontally moving sources continues the recent work of Howard, Malkus and Whitehead; and the slightly reformulated theory indicates behavior in qualitative agreement with the earlier work. The dynamics of slightly deformable heat sources is explored and a class of source aggregates whose strength decreases with depth

1. Introduction

This paper embraces convective behavior of a viscous fluid. The term “heat convection” was coined in the mid-nineteenth century to denote the transport of a fluid’s sensible heat by its own motion. Many suggested models of continental plate movement have contained the effect of convection, the heat arising from a fixed and sometimes unspecified source. This paper differs from most others, however, in that not only is the effect of convection included but the effect of movement or convection of explicitly stated heat sources is also included. As such, it continues the recent work of HOWARD, MALKUS and WHITEHEAD (1970), henceforth to be called HMW. The first part (section 2) involves some recent dynamical observations and calculations of heat sources free to move laterally; it is intended to show the effect and movements of possible concentrations of relatively radioactive regions of global dimensions near the surface of the Earth. The second part (section 3) involves analysis of the effect of a source lying in the upper region of a viscous fluid which is free to move vertically; it is intended to show the effect of crustal downwelling

is found to dynamically deform to an asymmetric shape which continues to propel the source. The consequence of downwelling which entraps heat-producing surface material is also reported. One of the principal features is a local deep heating which leads to an upward restoring force. Systems are discussed in which this causes an oscillating behavior with period $t \approx (\nu\rho C_p / (g\alpha Q_w))^\dagger$ which, if the Earth fulfills certain conditions, is of the order of a few hundred million years.

in the event that it entraps heat-producing materials.

In recent years, there has been an increasing amount of interest in continental drift, especially in association with the new global tectonics. Mechanisms to generate the associated mantle motions have centered around two principal energy sources. The first, relaxation of the Earth to a lower potential energy state, either relies upon relatively great amounts of stored potential energy being mechanically released at a slow rate, or it is coupled to some change in state within the Earth, either as a chemical process, a phase change, or gradual mean cooling of the Earth. The former process conflicts with the rapid fennoscandia uplift and the close approach to isostasy of the Earth’s field. The latter has often been suggested, but it requires significant chemical or physical transitions of great amounts of materials in order to supply the large amounts of energy associated with crustal motions over geological history.

If one assumes that the lowest strength regions of the mantle have a viscous character, the frictional energy to propel continental drift can be estimated by the formula $\mu U^2 A/L$. For example, if μ , the viscosity of the mantle, is 3×10^{21} poise and L , the depth of the layer with this minimum, is 500 km, the energy to make motions U of 4 cm/y is approximately 4.8×10^{18} erg/s or 1.2×10^{11} cal/s for an area A as large as the surface of the Earth. Thermodynamics dictates that such movements must arise from a mechanism which

* Publication No. 904, Institute of Geophysics and Planetary Physics, University of California, Los Angeles, Calif.

** Present address: Department of Physical Oceanography, Woods Hole Oceanographic Institution, Woods Hole, Mass. 02543, U.S.A.

is only partially efficient, and indeed the heat escaping from the Earth totalling approximately 3×10^{20} erg/s or 7.75×10^{12} cal/s is sufficiently great to inefficiently drive the above motion. It is worthy to note that if a mechanism which liberates 100 cal/g supplies this heat, and all material in the mantle of 9×10^{26} cm³ participates, with an average density of 4 g/cm³, it could persist for only 1.0×10^9 y before being exhausted. A major and energetic change of phase is necessary to supply 100 cal/g while chemical reactions of this magnitude are not usually associated with the relatively inert mantle material. However, a possible candidate might be the gradual cooling of an initially hot Earth.

Another source of energy is found in the radioactive release of slowly decaying uranium and thorium, which is found in granitic rocks and somewhat less in basalt. Although the amount of these trace elements varies from one particular type of rock to another, they generally demonstrate sufficient radioactivity (17×10^{-6} and 5×10^{-6} erg · cm⁻³ · s⁻¹, respectively; ALLEN 1964) to account for the present heat flux if extrapolated downward some 80 km. Although such an extrapolation has no observational basis, smaller depths of heat-producing material, of the order of 10 km, have been directly observed to contribute a significant amount of *local* heat flux, as discussed for instance by LACHENBRUCH (1968). Seismic studies indicate that typical granitic densities exist to the order of 30 km under continents, and basaltic densities exist to the order of 5 km under the ocean floor. The amount of radioactive materials below these depths is open to conjecture. On a global scale, the values of heat flux arising from the continents and the ocean floor have been remarkably similar. In conjunction with thermal conduction estimates similar to those used in the local studies, this fact has been used to argue against continental material supplying a significant amount of global heat. However, one could expect active convective motions to override conduction, make heat flux virtually uniform everywhere on the globe, and render conductive considerations of only local importance. This aspect of convection will be shown more fully in section 2.

Because of the uniformity of global heat flux some have felt compelled to extrapolate the heat flux measurements extending downward a few kilometers to deeper depths and have consequently suggested mantle

movements in the form of cellular convection. Many studies have been made of such motions; they exhibit a variety of forms, and generally become complex and even somewhat turbulent (KRISHNAMURTI, 1970a, b; WHITEHEAD, 1971) at the Rayleigh numbers greater than 10^5 , which are the values most widely suggested to exist in the Earth. This complexity does not appear to exist in the relatively simple plate tectonics which have recently emerged, as described, for instance, by LE PICHON (1968).

With lateral inhomogeneities present, the fluid no longer possesses the freedom to generate unconstrained convective cells, although if the inhomogeneity is very weak it may only alter the position or direction of the cells (SEGEL, 1969; NEWELL and WHITEHEAD, 1969). A mechanism involving a large insulating plate drifting upon small cellular convective motions has been suggested by ELDER (1968). It is not unlike the mechanism generated by lateral inhomogeneities discussed in HMW and in section 2. Documentation for stronger inhomogeneities is sparse. The calculations in HMW of a fluid close to the critical Rayleigh number and with a floating point heat source showed cellular features overlapping typical behavior of moving heat sources. The results showed that the lateral inhomogeneities always affected flow more strongly than the destabilizing gradient. Section 2 will assume that such inhomogeneities exist and are free to float in a uniform liquid.

In addition to the lateral changes in the top mantle due to the continents and their roots, a second striking feature of the outer layers of the Earth is a strong stratification. It is almost inevitable that radioactive heat producing materials are concentrated near the top of the mantle and are even more abundant in the crust. However, seismic studies have suggested that there is strong crustal downwelling under the oceanic trench regions. If this conveys significant heat producing materials to typical deep focus earthquake depths of a few hundred kilometers, deep local heating over geologic time would generate significant upthrusting forces. This aspect of heat source convection is discussed in section 3.

2. Self-propelling heat sources free to move laterally

This section will report upon experimental and theoretical studies of geometrically simple floating heat

sources which are free to move laterally. The emphasis will be upon the physics of the various processes which occur. If the Earth shares this physics, its added complexities will not greatly alter its behavior. It is a study of the type reported in HMW, which is a study of floating two-dimensional heat sources held at depth d in a fluid of depth h . In HMW the theoretical equations, although unwieldy to handle in general, were solvable in the limit of the heating parameter $R = g\alpha Qh^3/(\kappa^2\nu)$ small. The result indicated that the velocity was proportional to R . However, more intriguing was the fact that if the results were extrapolated to large R one found that the velocity became proportional to $R^{\frac{1}{2}}$ and that one lone heat source was capable of generating its own lateral motion. Experiments did not find this self-moving feature, although a variety of sources was observed to have a general $R^{\frac{1}{2}}$ behavior for large R . When the fluid was heated from below as well, velocities were found to be proportional to $R^{\frac{1}{2}}$ and R in various limits.

Here the theoretical problem will be solved in a slightly different way, and qualitative agreement will be found between experiment and theory. An $R^{\frac{1}{2}}$ law will result, and it will be shown to be a general feature of such convecting systems in the absence of heating from below. Complex floats with certain unique properties will also be reported upon.

We begin by defining the idealized system whose behavior can be expressed by the Boussinesq approximation to the equations of motion in which the variations of material properties with temperature and pressure have been ignored:

$$\mathbf{V} \cdot \mathbf{u} = 0, \quad (2.1)$$

$$\frac{D\mathbf{u}}{Dt} = -\rho^{-1}\nabla p + \nu\nabla^2\mathbf{u} - g\alpha T\hat{\mathbf{k}}, \quad (2.2)$$

$$\frac{DT}{Dt} = \kappa\nabla^2 T + Q\delta(x-a(x,t), z+d), \quad (2.3)$$

where $\mathbf{u}(x, z, t)$ is the velocity field, T the temperature, ν the kinematic viscosity, g the gravitational field in the direction of the unit vector $\hat{\mathbf{k}}$, α the volumetric coefficient of expansion, and κ the thermometric conductivity; δ is the Dirac delta function and represents a line source of heat at $x = a, z = -d$. Since a is a function of time, the source can move laterally. A "self-convection" condition to move the heat source

due to fluid motions by its own heating will be specified later. Basically, eqs. (2.1)–(2.3) are a good approximation to conservation of mass, momentum and energy, although the variation of fluid properties with temperature and pressure have been ignored except for volumetric expansion. However, in defense of eqs. (2.1)–(2.3) one must note that they contain the driving force for fluid motion ($g\alpha T\hat{\mathbf{k}}$), the friction opposing that force ($\nu\nabla^2\mathbf{u}$), and the effect of that motion (DT/Dt) in virtually the simplest general form possible.

We nondimensionalize as in HMW, scaling the variables upon the linear velocity for fixed a :

$$\psi = g\alpha\kappa^{-1}\nu^{-1}Qh^3\psi', \quad \delta = h^{-1}\delta',$$

$$r = hr', \quad t = h^2\kappa^{-1}t',$$

$$T = Q\kappa^{-1}T',$$

where primed coordinates are dimensionless, h is the depth of the fluid and ψ is the two-dimensional velocity potential,

$$u' = R\psi'_z, \quad w' = -R\psi'_x,$$

where $R = g\alpha\kappa^{-2}\nu^{-1}Qh^3$. Dropping the primes, the physics of the problem is expressed as

$$\sigma^{-1}\{\nabla^2\psi_t + R(\mathbf{u} \cdot \nabla)\nabla^2\psi\} + T_x = \nabla^4\psi, \quad (2.4)$$

$$T_t + R(\mathbf{u} \cdot \nabla T) = \nabla^2 T + \delta(x-a(t))\delta(z+d), \quad (2.5)$$

$$\sigma = \kappa^{-1}\nu,$$

in terms of the Prandtl number σ and the thermal Reynolds (Péclet) number R . Since σ in the interior of the Earth is generally of the order of 10^{24} or more, the terms with σ^{-1} can be ignored for our purposes. HMW ignored the $R(\mathbf{u} \cdot \nabla T)$ term to first order and found that by setting $\partial a/\partial t = R\psi_z(a, -d)$, solutions for the motion of the sources could be obtained such that $u \approx R$ for two floats parting in the limit of R small, which is a valid limit and $u \approx R^{\frac{1}{2}}$ for large R . Since for uniform motion $\partial T/\partial t$ is proportional to $R^{\frac{1}{2}}$ in that limit, it was not clear that the $R(\mathbf{u} \cdot \nabla T)$ term could be ignored. We will retain this term in the equation from the beginning by expanding the velocity in a Taylor series about the points where ∇T is expected to be greatest, that is, about any heat sources in the problems. We thus write in the convective term

$$\mathbf{u} = \mathbf{u}_s + ((x - \zeta_s) \cdot \nabla)\mathbf{u}_s + \frac{1}{2}((x - \zeta_s) \cdot \nabla)^2\mathbf{u}_s + \dots,$$

where ζ is the coordinate of source s , and then retain at most the first term which gives an asymmetry about the point s . This procedure is certainly valid in the local region where $x - \zeta_s$ is small, and can be expected to be valid also for larger $x - \zeta_s$ if no large velocity sign reversals are encountered which will turn the field around and sweep it the other way. Calling $u_s = U_s \hat{i} + W_s \hat{k}$, the thermal equation reads

$$T_t + RU_s \frac{\partial T}{\partial x} + RW_s \frac{\partial T}{\partial z} = \nabla^2 T + \delta(a_s, -d), \quad (2.6)$$

where we have condensed $\delta(x - a_s, z + d)$ to $\delta(a_s, -d)$.

Assuming that the heat source is moving uniformly to the right at velocity $\partial a_s / \partial t$, we transform coordinates to a moving frame $x = x - (\partial a_s / \partial t)t$. Defining $V \equiv R^{-1}(\partial a / \partial t)$, eq. (2.6) is rewritten

$$(-RV + RU_s) \frac{\partial T}{\partial x} + W \frac{\partial T}{\partial z} = \nabla^2 T + \delta(a_s) \delta(-d). \quad (2.7)$$

a_s is now a constant, and a constant flow is superimposed upon the flow field. The equation is now linearized except for the unknown quantities V and U_s ; if it is desired to understand the behavior of a number of heat sources, a separate thermal equation can be written for each source. The thermal field can be separated into components which are symmetric and antisymmetric in an x -direction about the heat source, and only the antisymmetric component generates a velocity U_s at its own source. The only antisymmetric operator is $\partial / \partial x$; the operators $W \partial / \partial z$ and ∇^2 are symmetric to a sign change in x . Therefore the operator $W \partial T / \partial z$ can be ignored. ∇^2 will be retained because its rejection would involve singularities caused by neglecting the highest order derivative. It also contains important thermal conduction behavior. In the limit $\sigma \rightarrow \infty$, the equations reduce to

$$\nabla^4 \psi = \frac{\partial T}{\partial x}, \quad (2.8)$$

$$(-RV + RU_s) \frac{\partial T}{\partial x} = \nabla^2 T + \delta(a_s, -d). \quad (2.9)$$

The above set of equations can be reduced to a set of algebraic relations for unknown V and U_s . This is accomplished by solving for $\psi(x, z, V, U_s)$ and then utilizing a "floatation" condition on the heat source (or sources) to determine U_s and V . Analysis proceeds

in the same manner as in HMW. General Fourier transforms of the temperature and velocity fields are calculated by defining

$$\theta(k, m) \equiv \int_{-\infty}^{\infty} e^{ikx} dx \int_{-1}^0 T(x, z) \sin(m\pi z) dz,$$

$$\phi(k, m) \equiv \int_{-\infty}^{\infty} e^{ikx} dx \int_{-1}^0 \psi(x, z) \sin(m\pi z) dz,$$

$$T(x, z) \equiv \pi^{-1} \int_{-\infty}^{\infty} e^{-ikx} dk \sum_{m=1}^{\infty} -\theta(k, m) \sin(-m\pi z),$$

$$\psi(x, z) \equiv \pi^{-1} \int_{-\infty}^{\infty} e^{-ikx} dk \sum_{m=1}^{\infty} -\phi(k, m) \sin(-m\pi z).$$

These are appropriate for nonslip-isothermal boundary conditions. Here ψ is the potential of flow caused by the thermal field and does not include the constant flow associated with the moving frame. The equations for the transforms are found by substitution into eqs. (2.8) and (2.9):

$$-ik\theta = (k^2 + m^2\pi^2)^2 \phi, \quad (2.10)$$

$$-iR(-V + U)k\theta + (k^2 + m^2\pi^2)\theta = -e^{ika_s} \sin(m\pi d). \quad (2.11)$$

Horizontal velocity at any point in the fluid due to the heat source at (a, d) is found by taking the inverse of eqs. (2.10) and (2.11):

$$\begin{aligned} \psi'_z(x, z) &= \sum_{m=1}^{\infty} \int_{-\infty}^{\infty} imk \exp[-ik(x - a_s)] \times \\ &\quad \times \sin m\pi d \cos m\pi z [(k^2 + m^2\pi^2)^3 + \\ &\quad + ikR(V - U_s)(k^2 + m^2\pi^2)^2]^{-1} dk. \end{aligned}$$

Recall that $U = R\psi'_z$, so that

$$\begin{aligned} U(x, z) &= \pi^{-4} R \sum_{m=1}^{\infty} m^{-3} \sin m\pi d \cos m\pi z \times \\ &\quad \times \int_{-\infty}^{\infty} \frac{ik \exp[-i\pi mk(x - a_s)]}{(k^2 + 1)^3 + ikv(k^2 + 1)^2} dk. \end{aligned} \quad (2.12)$$

This is the velocity in the fixed frame while $v \equiv (V - U_s)/(\pi m)$ is the velocity in the moving frame. When this equation is integrated, the series drops off rapidly for higher m and we need only analyze the harmonic $m = 1$. Calling $\pi(x - a) = \xi$,

$$U(x, z) = \frac{1}{4}\pi^{-3}R \sin \pi d \cos \pi z \times \left[\frac{(4+(2+\xi)v)e^{-\frac{1}{2}\xi}}{2v^2} - \frac{8 \exp[-\frac{1}{2}\xi(\sqrt{v^2+4}-v)]}{v^2 \sqrt{v^2+4}(\sqrt{v^2+4}-v)} \right]$$

for $\xi < 0$,

(2.13)

$$U(x, z) = \frac{1}{4}\pi^{-3}R \sin \pi d \cos \pi z \times \left[\frac{(4-(2-\xi)v)e^{\frac{1}{2}\xi}}{2v^2} - \frac{8 \exp[\frac{1}{2}\xi\sqrt{v^2+4}]}{v^2 \sqrt{v^2+4}(\sqrt{v^2+4}+v)} \right]$$

for $\xi > 0$,

(2.14)

which is the algebraic solution of the velocity of the fluid at the points (x, z) caused by a source moving with velocity V . In the case of $\xi = 0$, the formulae reduce to

$$U(a, z) = \frac{1}{2}\pi^{-3}Rv\{\sqrt{v^2+4}(2+\sqrt{v^2+4})\}^{-1} \times \sin \pi d \cos \pi z. \quad (2.15)$$

A floatation or self-convection condition will define V as a function of $U_s(x, z)$, and will essentially close the equations so that solutions can be obtained. The behavior of various floats consisting of heat source aggregates can be found using the appropriate floatation conditions. Some examples follow.

2.1. Various geometries

2.1.1. *Point source being dragged with velocity V through a fluid.* This simplest case has $V = \text{constant}$ and we find $v = (V - U_s)/\pi$. Eq. (2.15) reads

$$U_s = U(a, -d) = \frac{1}{4}\pi^{-3}Rv\{\sqrt{v^2+4}(2+\sqrt{v^2+4})\}^{-1} \times \sin 2\pi d \quad (2.16)$$

For small v , the solution is

$$U_s = \frac{1}{32}\pi^{-4}R(V - U_s) \sin 2\pi d,$$

i.e.

$$U_s = V(1 - 32\pi^4 R^{-1} \sin^{-1} 2\pi d),$$

and for large R ,

$$U_s = V[1 - O(R^{-1})]. \quad (2.17)$$

This implies that v is small when R is large. When the terms $(v^2+4)^{\frac{1}{2}}$ become important, a solution exists for $V \gg U_s$,

$$U_s = \frac{1}{4}\pi^{-2}RV^{-1}, \quad (2.18)$$

and drops off as V increases.

By equating eq. (2.17) to eq. (2.18) we find that the two solutions intersect when

$$V = (\frac{1}{4}\pi^{-2}R \sin 2\pi d)V^{-1},$$

or, for $d = \frac{1}{4}$,

$$V = \frac{1}{2}\pi^{-1}R^{\frac{1}{2}}. \quad (2.19)$$

For small R , if we assume $U_s \ll V$, then $v = V/\pi$ and

$$U_s = \frac{1}{32}\pi^{-4}RV \sin 2\pi d, \quad \text{for small } V, \quad (2.20)$$

$$U_s = \frac{1}{4}\pi^{-1}RV^{-2} \sin 2\pi d, \quad \text{for large } V, \quad (2.21)$$

Since R is small, this obeys the assumption $U_s \ll V$. The limits join at the value $V = \pi$, at which point

$$U = \frac{1}{4}\pi^{-3}R \sin 2\pi d,$$

which is small. The behavior for the limiting cases of large and small R is sketched on fig. 1a.

This problem was readily duplicated in the laboratory by towing a tightly stretched stainless steel wire horizontally through viscous oil 4 cm deep. The wire was sufficiently fine (0.001 inch) to contribute only negligible stress to the fluid. The oil used was 500 centistoke ($\nu = 5 \text{ cm}^2/\text{s}$) silicon oil with a volume coefficient of expansion α of $0.00108 \text{ }^\circ\text{C}^{-1}$ and a thermometric conductivity κ of $0.001 \text{ cm}^2/\text{s}$. The stainless steel wire had a resistance of $17 \text{ } \Omega/\text{cm}$ and a range of R from

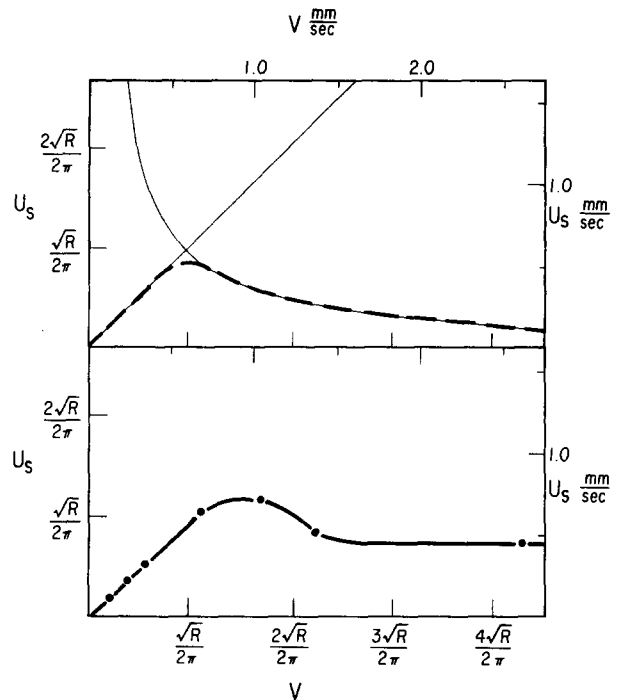


Fig. 1. Sketch of the predictions of eqs. (2.17)–(2.19) in the upper picture (a) compared with experimental datum points (b) for the fluid velocity at a point source for $R = 900000$.

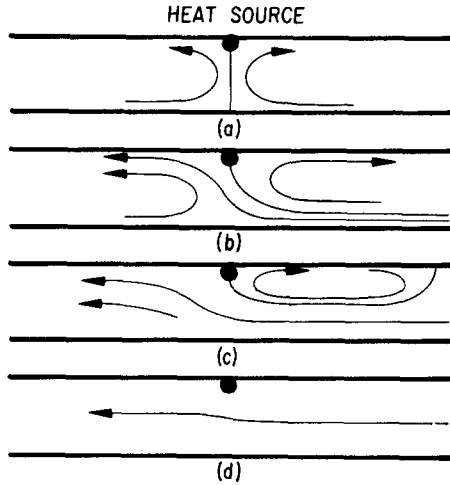


Fig. 2. Streamlines of flow in the frame of a single point heater at large R moving through a fluid with velocity V . (a) $V = 0$; (b) $V = 0.066R^{1/2}$; (c) $V = 0.17R^{1/2}$; (d) $V = 0.36R^{1/2}$.

10^3 to 10^6 was experimentally observed. The velocity of the oil at the surface above the heater was measured by timing the transit time of 1 mm polyethylene floats over a 5 mm distance. A typical plot of U_s versus V is shown in fig. 1. Within an experimental accuracy of 5% it was seen that U_s never got as large as V , while for large R there was a region where $U_s = V$ before dropping off at a value of $U_s = 0.2R^{1/2}$. This qualitative behavior is compatible with the theoretical predictions. Streamlines of the flow were determined by observing the trajectories of neutral density floats. The results are shown in fig. 2. The flow is split into two closed branches which decrease with increasing V . The forward branch vanished at $V = 0.2R^{1/2}$, which is close to the theoretical estimate eq. (2.19).

A case of $U_s > V$ was not admitted by eq. (2.16) and also was never seen in this experiment. This implies that such a freely floating isolated heat source would not selfconvect. However, a source with a small asymmetry in its shape would be expected to climb the $U-V$ curve in fig. 1 until U_s drops off, which occurs at $U_s \approx R^{1/2}$.

2.1.2. *Two overlying connected point heat sources.* If two heat sources are connected so that one lies at a depth d_1 and another lies at depth d_2 , of strengths R_1 and R_2 respectively, each will make a thermal tail for the other. If we solve for the velocity at any point from two such heaters we find

$$U(x, z) = \frac{1}{2}\pi^{-3}R_1v_1\{\sqrt{v_1^2+4}(2+\sqrt{v_1^2+4})\}^{-1} \times \sin \pi d_1 \cos \pi z \quad (2.22)$$

$$+ \frac{1}{2}\pi^{-3}R_2v_2\{\sqrt{v_2^2+4}(2+\sqrt{v_2^2+4})\}^{-1} \times \sin \pi d_2 \cos \pi z,$$

where

$$v_1 \equiv (V-U_1)/\pi, \quad v_2 \equiv (V-U_2)/\pi,$$

with

$$U_1 = U(a, d_1), \quad U_2 = U(a, d_2).$$

If the two heaters have equal drag in the fluid, the speed of the float will be the mean of U_1 and U_2 , so the floatation condition is $V = \frac{1}{2}(U_1+U_2)$. We can now define v_1 and v_2 as

$$v_1 = (V-U_1)/\pi = \frac{1}{2}(U_2-U_1)/\pi,$$

$$v_2 = (V-U_2)/\pi = \frac{1}{2}(U_1-U_2)/\pi,$$

and therefore

$$v_2 = -v_1.$$

Using eq. (2.22) and the above definitions, we find

$$v_1 = \frac{1}{2}(U_1-U_2)/\pi = \frac{1}{4}\pi^{-4}R^*v_1\{\sqrt{v_1^2+4}(2+\sqrt{v_1^2+4})\}^{-1}, \quad (2.23)$$

where

$$R^* = (R_1 \sin \pi d_1 - R_2 \sin \pi d_2)(\cos \pi d_1 - \cos \pi d_2).$$

The solution is shown in HMW as

$$v_1^2 = \{(\frac{1}{4}\pi^{-4}R^* + 1)^{\frac{1}{2}} + 1\} \{(\frac{1}{4}\pi^{-4}R^* + 1)^{\frac{1}{2}} - 3\}. \quad (2.24)$$

This has a solution for nonzero v_1 when $R^* > 32\pi^4$ and then we expect self-propulsion such that for large R^*

$$v_1 = \frac{1}{2}\pi^{-2}\sqrt{R^*}. \quad (2.25)$$

The velocity of the heat source V is now readily calculated by finding U_1 from eq. (2.22) and using $V = v_1 + U_2$. This yields, for R^* large,

$$V = \frac{1}{2}\pi^{-1}\sqrt{R^*} + O(R^{*-1}).$$

In contrast to the single point heat source, this pair of sources will exhibit self-convection if R^* is positive and sufficiently large. Examination of R^* shows that R^* is positive only if the lower heater R_2 is greater than

$R_1 \sin \pi d_1 / \sin \pi d_2$. The physical meaning of this requirement is shown on fig. 3. The thermal field of the lower float is swept in one direction, while the field of the upper float goes in the other. If the lower thermal field is sufficiently strong, its thermal tail keeps the source moving.

A similar analysis can simulate a body whose rigidity is somewhat above the center of heating. If the upper heater is powerless and possesses much greater drag than the lower float, then the floatation condition is $V = U_1$, $R_1 = 0$ and $v_2 = (U_1 - U_2) / \pi$. Using eq. (2.22),

$$U_1 = -\frac{1}{2}\pi^{-3}R_2v_2\{\sqrt{v_2^2+4}(2+\sqrt{v_2^2+4})\}^{-1} \times \sin \pi d_2 \cos \pi d_1,$$

$$U_2 = -\frac{1}{2}\pi^{-3}R_2v_2\{\sqrt{v_2^2+4}(2+\sqrt{v_2^2+4})\}^{-1} \times \sin \pi d_2 \cos \pi d_2,$$

we find

$$v_2 = U_1 (\cos \pi d_1 - \cos \pi d_2) / (\pi \cos \pi d_1).$$

The solution of large U_1 is therefore

$$\begin{aligned} U_1 &= \cos \pi d_1 \{R \sin \pi d_2 (\cos \pi d_1 - \cos \pi d_2)\}^{\frac{1}{2}} \\ &\quad \times \{2\pi (\cos \pi d_1 - \cos \pi d_2)\}^{-1} \\ &= \frac{1}{2}\pi^{-1}R^{\frac{1}{2}} \cos \pi d_1 \sin^{\frac{1}{2}}\pi d_2 (\cos \pi d_1 - \cos \pi d_2)^{-\frac{1}{2}}. \end{aligned} \quad (2.26)$$

A float with this property was experimentally observed. The upper body was a $2 \times 1 \times 50 \text{ cm}^3$ styrofoam float which was placed in a $60 \times 60 \text{ cm}^2$ tank filled 4 cm deep with 500 centistokes oil. The lower heater was a 0.001 inch diameter stainless steel heating wire stretched below so that the wire was at 3.0 cm depth. Two soft copper wires were hung loosely to the float from above to feed in electrical power, while massive copper counterweights at each end of the wire kept the styrofoam almost totally immersed and guarded against any self-propulsion from tipping of the float.

The float exhibited an immediate and decided tendency to propel itself as soon as the heater current was turned on. A small push in either direction was sufficient to generate a preferred direction of motion. Time-lapse movies taken of the float show it moving to the right at a constant rate, being stopped by a bumper near the end of the tank, then starting back the other way. This process can be repeated for many traverses of the tank.

Movies and pictures taken from the side through the

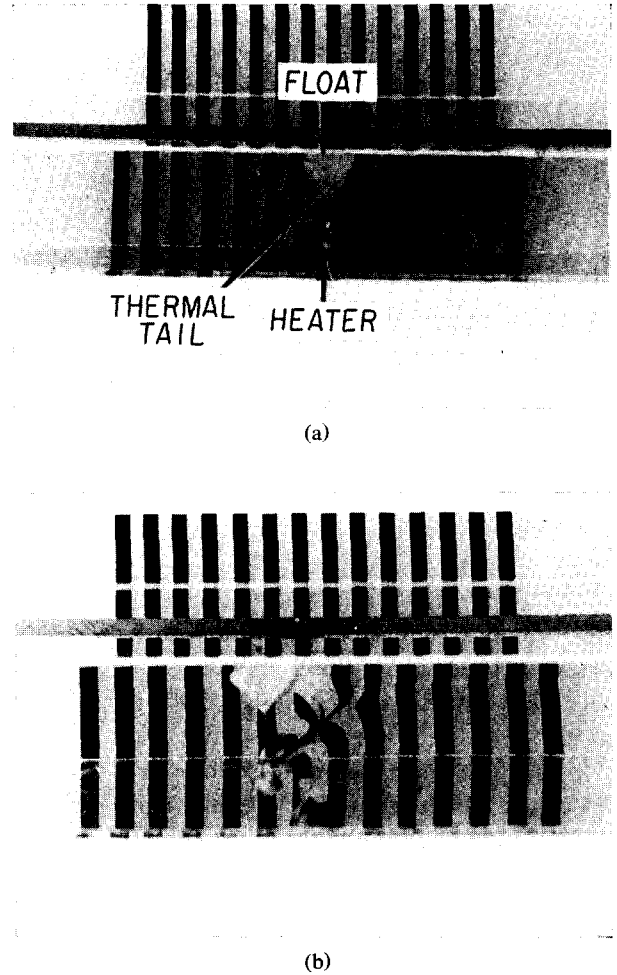


Fig. 3. Photograph of a self-propelling source moving (a) to the right, (b) to the left. The background stripes are bent by the intense thermal field which streams aft of the float.

oil, as shown in fig. 3, demonstrate the dynamic asymmetry of the thermal field as it trails behind the float. One can calculate the predicted rate of flow for such a device with

$$\begin{aligned} d_1 &= 1.0/4.0, \quad d_2 = 3.0/4.0, \\ U_1 &= 2^{-9/4}\pi^{-1}R^{\frac{1}{2}} = 6.7 \times 10^{-2}R^{\frac{1}{2}}. \end{aligned} \quad (2.27)$$

Since the apparatus travelled at a constant speed, it was possible to measure the velocity to an accuracy of better than 5% at different values of R . The measurements showed a striking $R^{\frac{1}{2}}$ dependence. A second apparatus was made at one-fourth the size of the first to get additional readings at low R and the data overlapped well. As shown in fig. 4, these data, taken before

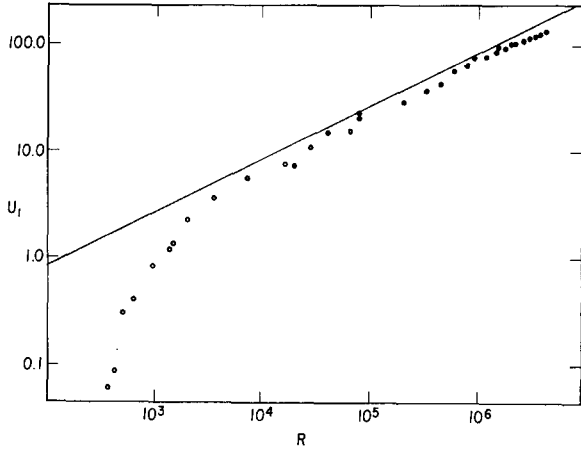


Fig. 4. Data for the speed of the self-propelling float versus R as compared to eq. (2.27), $U_1 = 7.97 \times 10^{-2} R^{1/2}$. Data with open circles were taken in a $\frac{1}{4}$ -sized apparatus compared to data with closed circles.

the theoretical reformulation of the basic equations was completed, agree closely with eq. (2.27) in not only the $R^{1/2}$ power law but also closely with the coefficient.

In addition, the experiment exhibited a drop-off in velocity at small values of R ("small" being less than 10^3). At such values, the thermal tail was seen to be very small; the most dramatic decrease in velocity was seen when the tail was so small that the thermal field essentially brushed the float above.

2.1.3. Self-deformable bodies. A network of sources attached to each other in such a way that the network can slowly deform under forces in the system can be envisioned as a model of more continuous heat-producing bodies. For example, if a heat source gets slightly softer with depth, the deformation would take the same direction as the thermal tail shown in fig. 6, and as discussed in the model above. It would thus produce an asymmetric body.

Another configuration which dynamically deforms into an asymmetric body is the field of three point-heat sources at depth d and separated from each other by the distance a . Let the two outer bodies be rigidly connected to each other and let the inner body be unattached to the other two, as in fig. 5a, b. In the limit of v small for each source, eq. (2.13) reads

$$U = \frac{1}{4}\pi^{-4}R \cdot \frac{1}{4}\left(\frac{1}{2}\xi\right)\left(1 + \frac{1}{2}\xi\right)e^{-\frac{1}{2}\xi}. \quad (2.28)$$

The velocity of fluid from the three sources is shown in fig. 5a, b for the sources being far apart (far field) and close together (near field), respectively. Note that in the far field limit, the net velocity on either side of the central float is inward, and if the central float is slightly perturbed it will be restored to the center by the flow of the outside floats, thus restoring the three-float aggregate into a symmetric body. In the near field limit, however, the net fluid velocity on either side of the central float is outward, and if the central float is slightly deflected it will get swept into a branch of flow which moves it away from the center, thus deforming the three-float aggregate into an asymmetric body. Unfortunately, the two outer bodies must be closer than twice the depth of the fluid for the near field limit to apply. Experiments at heating rates of $R = 3 \times 10^5$, and theoretical development of eq. (2.14) in the limit of large v , indicate that the heaters may even have to be closer in the large R limit. Since the Earth-like crustal plates are generally more extensive than the presumed depths of low viscosity, this mechanism would not be expected to be globally relevant.

More extensive arrays of heaters also have interesting self-deforming properties. Take, for instance, an array of sources as shown in fig. 5c. Due to the presence of the heaters, a large circulation upwells under the center of the float and sweeps heat laterally. If this velocity varies sufficiently slowly, it can be assumed that this occurs at the constant velocity v . To see the behavior for large v , we find that eq. (2.13) reads, for a point source,

$$U = \frac{1}{8}\pi^{-3}R \sin \pi d \cos \pi z \\ \times \frac{1}{2}v^{-2} \left\{ (2 + |\xi|) \exp \left[-\frac{1}{2}|\xi| \right] - 8 \exp \left[-\frac{1}{2}|\xi|/|v| \right] \right\} \quad (2.29)$$

for ξ and v in the same direction, i.e. $\xi \cdot v > 0$, and eq. 2.14 reads

$$U = \frac{1}{8}\pi^{-3}R \sin \pi d \cos \pi z \\ \times \frac{1}{2}v^{-2} \left\{ (-2 + |\xi|) \exp \left[-\frac{1}{2}|\xi| \right] - 8 \exp \left[-|\xi|/|v| \right] \right\} \quad (2.30)$$

for $\xi \cdot v < 0$. Note that the circulation dies out when $\xi = O(1)$ in the upstream direction, but only when $\xi = O(v)$ in the downstream direction. This occurs as a consequence of the thermal field being moved downstream; therefore the flow at any given point is produced only by those heaters closer to the center.

Assuming each heater is of the same magnitude, and

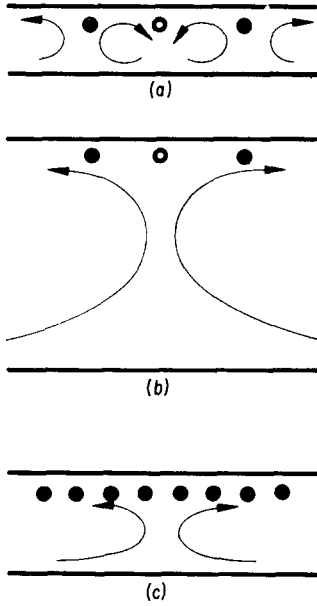


Fig. 5. Sketches of source aggregates in (a) the near field limit (b) the far field limit; (c) a deformable simulation of a continuous slab.

numbering the heaters consecutively, the velocity is calculated from eq. (2.29) as

$$\begin{aligned}
 U_2 &= \frac{1}{4}\pi^{-3}Rv^{-2}(e^{-\xi/(2v)}), \\
 U_3 &= \frac{1}{4}\pi^{-3}Rv^{-2}(e^{-\xi/(2v)} + e^{-2\xi/(2v)}), \\
 U_4 &= \frac{1}{4}\pi^{-3}Rv^{-2}(e^{-\xi/(2v)} + e^{-2\xi/(2v)} + e^{-3\xi/(2v)}), \\
 &\vdots \\
 U_n &= \frac{1}{4}\pi^{-3}Rv^{-2} \sum_{m=1}^n e^{-m\xi/(2v)}.
 \end{aligned}$$

With extension of the heater proportional to $U_n - U_{n-1}$, it is clear that maximum extension occurs in the center of the float, and decreases outward at the rate $e^{-x/(2v)}$. For large v , this means that U_n varies slowly and our initial assumption of constant v is valid. In the Earth, if $U = 10^{-7}$ cm/s, the plate is 10000 km half-width and $\kappa = 10^{-3}$ cm²/s, the depth would have to be less than 30 km for a stress to vary by a factor of 2.7. For $h = 10^7$ cm, we find $v = 10^3$ which is large. Therefore the assumption of slowly varying lateral stress would appear to be useful for Earth studies.

This lateral motion also smears out the thermal field. To see this, one can directly integrate eq. (2.11) for the thermal field, and end up with terms proportional to $ve^{-\xi/(2v)}$ in the downstream direction and $v^{-1}e^{-\xi v}$ in the upstream direction for each individual

heater. Therefore, one would again expect that extended sources of the size of continents would generate motions which would spread out heat flux and make it almost uniform over the entire globe unless h were less than 30 km.

2.2. Discussion of the formulation and applications

The principal aim was to rederive eqs. (2.8) and (2.9) in algebraic form, from which the behavior of more complicated heaters is readily calculated, and then to discuss specific models. In the same vein, SMITH (private communication) has been investigating the case of multiple and purposely asymmetric heat sources. It is quite conceivable to even extend the analysis to continuous systems using eqs. (2.8) and (2.9) as solutions to a Green's function; the equations, being linear, admit superposition of solutions.

Adopting the operator $U_s \partial T / \partial x$ resembles the Oseen approximation used in the Navier-Stokes equations. To be valid, the leading term must retain the most significant physics. If so, an investigation of the neglected terms illuminates additional physics but does not lead to new results, only small corrections. The term $W \partial T / \partial z$ expresses the vertical convection of heat by the fluid. In the experiment discussed in section 2.1.1, in which a single heat source was towed through a viscous fluid, a thermal plume was observed to surge up to the surface where heat was then conducted to the outside. The upward motion of such a plume is evident in fig. 3; however, it erased the thermal-tail effect only slightly. In fact, the operator $W \partial T / \partial z$ lacks the necessary asymmetry in the horizontal direction to counteract the thermal-tail effect and can only dilute it.

For a freely floating point source of heat, U_s is equal to V , and the term $(U_s - V) \partial T / \partial x$ is identically zero. The next-order term in the x -direction is $(x - s) (\partial U_s / \partial x) (\partial T / \partial x)$. This operator is symmetric fore and aft of S and so does not generate a dynamic asymmetry but instead convects fluid either toward or away from the float in a symmetric manner. In regions of upwelling, $\partial u / \partial x$ is positive near the top surface to conserve mass and so the fluid motion conveys heat out away from the heat source, as the near field flow did in fig. 5c. This feature was observed in many of the experiments described in section 2.1.1, and can be responsible for spreading the heat flux over a very wide region.

At the risk of over-emphasis, we repeat that this

model contains the complete dynamical story of an idealized floating heat source. As such, the sources of thermal energy (the heat source), and kinetic energy (the operator $g\alpha\partial T/\partial x$), and the sink of thermal energy (isothermal surfaces) and kinetic energy (viscosity) are explicitly stated. It can be expected that features of this model will persist even if accompanied by physical processes which do not greatly change the energy balance. For instance, if significant variations in strength of the carrier fluid are expected, as present Earth models suggest, the rate of deformation of different levels can be parameterized as self-deformation as done in section 2.1.3. This could be done for vertical as well as horizontal aggregates of sources, viscously or plastically held together.

A central feature of the solutions presented in this section is the velocity being proportional to $R^{\frac{1}{2}}$ for large R . This is in fact a general property of these formulations as can be seen by writing eqs. (2.4) and (2.5) in scaling form, assuming that derivatives are order one:

$$\psi + T = 0, \quad (2.31)$$

$$R\psi T = T + 1. \quad (2.32)$$

We solve for ψ and get

$$R\psi^2 + \psi - 1 = 0, \quad (2.33)$$

with the solution

$$\psi = (-1 \pm \sqrt{1+4R})/(2R). \quad (2.34)$$

Since $U = R\psi$ by definition, we solve eq. (2.34) for large R to get

$$U = O(R^{\frac{1}{2}})$$

Such $R^{\frac{1}{2}}$ behavior also emerges from boundary layer studies of cellular convection with rigid boundaries; see, for instance, ROBINSON (1967).

When applying this $R^{\frac{1}{2}}$ law to the Earth, one encounters large uncertainties in the values of viscosity and depth of fluid, and hence the question of whether this theory predicts drift velocities of 4 cm/y has little meaning. However, there is some merit in using the more reliably known quantities to determine bounds upon the unknown quantities. For this purpose, we use the values $U = 10^{-7}$ cm/s, $g = 980$ cm/s², $\alpha = 2 \times 10^{-5}$ °C⁻¹, $\kappa = 0.01$ cm²/s and $Q = 2 \times 10^3$

TABLE 1

Viscosity as a function of depth of the low viscosity layer deduced by using eq. (2.19) as discussed at the end of section 2

ν	h (km)
10^{19}	1
10^{21}	100
3×10^{21}	300
10^{22}	1000

°C · cm²/s. Q was determined by assuming that seven Earth plates, each with a line heat source 10000 km long, supply the entire heat flux emerging from the Earth. Putting these values into eq. (2.19), we then see that $\nu/h = 10^{14}$. Since ν and h are relatively poorly known for the Earth, we present various values of these quantities in table 1. The third pair down, $\nu = 3 \times 10^{21}$ cm²/s and $h = 300$ km, was found by MCCONNELL (1968) to give the best fit to the spectral observations of the uplift of Scandinavia.

3. Vertical convective entrainment

The asymmetries discussed so far have arisen from horizontal motions manifested by the term $U\partial T/\partial x$ in the differential equations. However, geometries exist where such terms are intimately coupled with vertical motions which lead to horizontal asymmetries. A common example is the Bénard convective problem in which heat is transported laterally to hot thermals

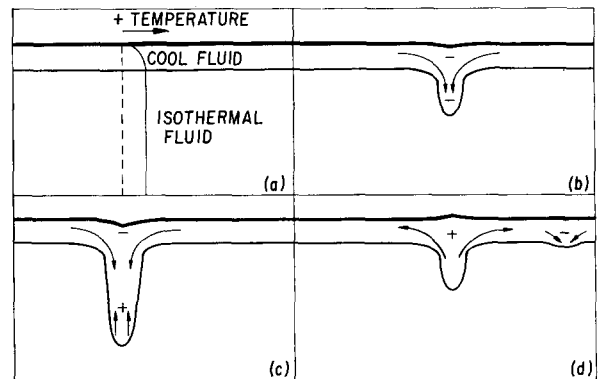


Fig. 6. Consequences of vertical entrainment of heat sources. (a) The temperature distribution produced by a layer of uniform heat-generating material above an isothermal fluid, (b) initial downwelling of cool surface material; (c) deep upthrusting caused by long-time scale internal heating; (d) upwelling of hot, superheated material. Plus or minus signs indicate temperature excess or deficiency with respect to isothermal material.

which then take the heat to the surface. When a heat source is trapped in downwelling thermals, an interesting behavior can result.

A model which clearly illustrates this process consists of a layer of heat-producing material overlying a deeper layer of fluid, as shown in fig. 6. Boundary conditions are such that the same amount of heat is removed at the top boundaries as is produced by the heat-producing material, so that the internal fluid below, in a motionless state, is isothermal. Both deep and top materials are presumed to have the same properties. It is assumed that the density is dependent upon temperature in the form $\rho = \rho_0(1 - \alpha T)$ so that the top layer is unstable and tends to sink.

Examination of a local region where the flow downwells in fig. 6 shows that the material heats up as it descends. The change in the downward force per unit length of slab changes at the rate

$$\frac{\partial F}{\partial t} = -\rho_0 g \alpha w \frac{\partial \bar{T}}{\partial t}, \quad (3.1)$$

where $\rho_0, g, \alpha,$ are defined previously, w is the width of the plunging slab, and

$$\bar{T} \equiv \int_{-z}^0 T(z') dz'$$

is the average temperature of the descending slab in deviation from an isothermal state. The slab extends down into the fluid to a depth z . Its time derivative is not dependent upon the details of the heating process, for we note that $\partial T(z')/\partial t = Q/(\rho C_p)$, a constant, for $z' < z$, and $\partial T(z')/\partial t = 0$ for $z' > z$. Therefore

$$\begin{aligned} \frac{\partial \bar{T}}{\partial t} &= T(z) \frac{\partial z}{\partial t} + \int_{-z}^0 \frac{\partial T(z')}{\partial t} dz' \\ &= -T_0 \frac{\partial z}{\partial t} + \frac{Q}{\rho C_p} z, \end{aligned}$$

where ρC_p is the specific heat per unit volume and T_0 denotes the average temperature of the material which turns downward into the slab. The rate of change of the buoyancy force is therefore

$$\frac{\partial F}{\partial t} = -\rho_0 g \alpha w L \left(T_0 \frac{\partial z}{\partial t} - \frac{Qz}{\rho C_p} \right). \quad (3.3)$$

A viscous force resists motion and is proportional to $\mu D L h^{-1}(\partial z/\partial t)$, where D is the distance between the plunging segments and h is the depth of the fluid; it

has been assumed that $D \gg h$. Equating the rate of change of this to $\partial F/\partial t$ and rearranging, we get

$$\frac{\partial^2 z}{\partial t^2} - \lambda \frac{\partial z}{\partial t} + \omega^2 z = 0, \quad (3.4)$$

where

$$\lambda = \frac{g \alpha w h T_0}{\nu D}, \quad \omega^2 = \frac{g \alpha w h Q}{\nu D \rho C_p}.$$

The solution is now proportional to e^{pt} , where

$$p = \frac{1}{2}(\lambda \pm \sqrt{\lambda^2 - 4\omega^2}). \quad (3.5)$$

If $\omega^2 > \frac{1}{4}\lambda^2$, p will be complex, hence the model will oscillate with a period

$$t_0 = 2\pi(\omega^2 - \frac{1}{4}\lambda^2)^{-\frac{1}{2}}, \quad (3.6)$$

and grow with time

$$t_g = 2\lambda^{-1}. \quad (3.7)$$

In order to have oscillations, the condition

$$\frac{g \alpha w h \rho C_p T_0^2}{4 \nu D Q} < 1 \quad (3.8)$$

must be satisfied. The same condition is derived in a more complete stability problem in the appendix. Although this condition can be satisfied under certain circumstances in the Earth, laboratory models which fit this criterion and still have relatively large amplitudes have not been found.

One finds that only very viscous fluids will oscillate with a period slow enough to allow significant heating of the plunging material. A fluid with $\nu = 10^2 \text{ cm}^2/\text{s}$, which is ten times the viscosity of temperate honey, in association with an internal heat source of 0.01 W/cm^3 will have a period of 10 min. To keep shear energy production to a fraction of the driving energy, the total downward displacement of the unstable fluid would have to be less than 10^{-3} cm . This is considerably less than the amplitudes necessary for the equations to be valid, although a subsequent analysis will show that the same process occurs for vanishingly small amplitudes. Greater heat production yields faster oscillations but only slightly larger amplitudes. Note that the growth rate λ is proportional to αT_0 , which is essentially a measure of the density imbalance of the surface fluid over the interior. Present experimental efforts are aiming at producing a surface fluid which is slightly

heavier than the interior fluid and which is electrically conductive.

Even in this primitive form, eq. (3.4) represents the dynamics of a system in energetic equilibrium as well as in force equilibrium. The potential energy represented by heat produced by the material is removed by conduction at the top surface, the heat deposited in the interior being convected upward in the up-cycle.

The force within the plunging slab is proportional to the local temperature excess as shown in fig. 6. The material is under tension as the slab begins its plunge, becomes compressive near the bottom of the slab at a later time, is increasingly compressive over most of the slab later, which generates the restorative upwelling, and is entirely compressive as the slab surges upward and restores the heat-producing material to the surface.

The preceding analysis has assumed a geometric form for the fluid motion, clearly a dangerous procedure. The system can fortunately be recast into a form which sacrifices geometric and physical simplicity for mathematical convenience so that a more thorough analysis of the equations of motion can be done. As shown in the appendix, this admits an analysis using expansion procedures akin to those used extensively in stability theory.

Basaltic rock, lining the ocean floor, is seen to accompany the sea floor as it spreads away from ocean ridges (MAXWELL *et al.*, 1970), and is also seen to exist near the downwelling trenches, which show evidence of dynamic activity to depths of 700 km (OLIVER and ISACKS, 1967). If heat-producing material accompanies ridge upwelling and lithospheric plunging to significant depths, local heating could be expected to produce forces whose rate of change would be expressible as a second-order differential equation in time, similar to eq. (3.4), whose solution, in general, can involve oscillations. To see the magnitude of the various terms in a possible Earth-like model, we use $\rho C_p = 0.6 \text{ cal} \cdot \text{cm}^{-3} \cdot \text{s}^{-1}$, $\nu = 10^{21} \text{ cm}^2/\text{s}$, $h/D = 0.1$, $g = 10^3 \text{ cm/s}^2$, $\alpha = 10^{-5} \text{ }^\circ\text{C}^{-1}$, $k = 6 \times 10^{-3} \text{ cal} \cdot \text{cm}^{-2} \cdot \text{s}^{-1}$, and estimate T_0 from the conductivity relation

$$T_0 = \frac{1}{24} Q w^2 / k, \quad (3.9)$$

which is the average temperature of a thin layer with source Q , of thickness $\frac{1}{2}w$ and insulated on one side. For Q of the order of basaltic rocks ($= 1.2 \times 10^{-13} \text{ cal} \cdot \text{cm}^{-3} \cdot \text{s}^{-1}$), the parameter group $g\alpha h\rho C_p Q /$

$(24^2 \cdot 4k^2 \nu D)$ is 0.86×10^{-36} . To satisfy the oscillation condition eq. (3.8) we then must have

$$w^5 < 11.6 \times 10^{35} \text{ cm}^5,$$

or

$$w < 1.63 \times 10^7 \text{ cm} = 163 \text{ km}.$$

If the Earth were originally covered with 60 km of material with the above heat productivity, eqs. (3.6) and (3.7) indicate that the motion would grow with an exponential growth time of $750 \times 10^6 \text{ y}$ and oscillate with a period of $260 \times 10^6 \text{ y}$. Note that eq. (3.9) essentially makes the growth time a sensitive function of w while the oscillation time remains relatively insensitive.

If the basalt underlying the ocean sediments is significantly less than 60 km deep, the heat produced by such a source is much smaller than that which is observed to escape from the Earth. In that case, the principal energy source of continental drift might be heat from the continental material. The oscillatory mechanism discussed in this section would be closely related to the situation which would occur if a continent overrides a downwelling trench region, for then very large amounts of heat-producing material could be suddenly entrapped. This would lead to rapid deep heating, upwelling forces within the trench and a sudden alteration in the relative motion of the adjacent lithospheric plates. Assuming that the newly entrapped radioactive material is lighter than the ocean crust, the time it takes for this flow inversion to take place would be less than half the oscillatory period of eq. (2.6). If a heating material were seven times as radioactive as the basaltic value of $1.2 \times 10^{-13} \text{ cal} \cdot \text{cm}^{-3} \cdot \text{s}^{-1}$, the rebound time would be less than $75 \times 10^6 \text{ y}$.

Much more rapid reversal times could be expected if relatively light, continental material overrode a trench and became entrapped. When this happens, the coefficient λ in eq. (3.4) will suddenly decrease and even reverse sign. One could then get a balance between the first two terms in eq. (3.4), and if the newly entrapped material is 10% lighter than the deep mantle, the upwelling time will be estimated by the time

$$t = \frac{\nu D \rho}{g \omega h \Delta \rho} = 5 \times 10^5 \text{ y},$$

using $\nu = 10^{21} \text{ cm}^2/\text{s}$, $h/D = 0.1$, $D = 60 \text{ km}$, and $g = 10^3 \text{ cm/s}^2$. It is possible that such a process and its

rebound is connected with mountain building episodes.

Appendix. The stability problem

The system in section 3 can be recast into a theoretically more tractable problem. We will look at the stability of a layer of fluid heated from below with a constant heat source gradient γ in the fluid such that the motionless system obeys the conductive law

$$\kappa \frac{\partial^2 T_0}{\partial z^2} + \gamma z = 0,$$

with the solution

$$T_0 = \beta z + \frac{1}{8}\kappa^{-1}\gamma(\frac{1}{8}z - z^3), \quad (\text{A.1})$$

where z is positive in the direction of gravity and is zero at the midplane. The Boussinesq equations of conservation of mass, momentum, energy and heat source are now

$$\nabla \cdot \mathbf{u} = 0, \quad (\text{A.2})$$

$$\frac{\partial \mathbf{u}}{\partial t} + \mathbf{u} \cdot \nabla \mathbf{u} = \rho^{-1} \nabla p + \nu \nabla^2 \mathbf{u} - g\alpha T \hat{\mathbf{k}}, \quad (\text{A.3})$$

$$\frac{\partial T}{\partial t} + \mathbf{u} \cdot \nabla T + (\beta - \frac{1}{2}\kappa^{-1}\gamma \hat{z}^2)w = \kappa \nabla^2 T + Q, \quad (\text{A.4})$$

$$\frac{\partial Q}{\partial t} + \mathbf{u} \cdot \nabla Q + \gamma w = 0, \quad (\text{A.5})$$

where $\hat{z}^2 = \frac{1}{24} - z^2$. Defining $W \equiv g\alpha\beta h^3/\nu W'$, $T = \beta h T'$, $Q = \kappa\beta h^{-1} Q'$, $\mathbf{x} = h\mathbf{x}'$ and $t = \kappa^{-1}h^2 t'$ (dropping the primes) and taking $\nabla \times \nabla \times (\text{A.3})$, the linearized dimensionless equations become

$$\left(\sigma^{-1} \frac{\partial}{\partial t} - \nabla^2\right) \nabla^2 W + \nabla_1^2 T = 0, \quad (\text{A.6})$$

and defining $R_a = g\alpha h^4 \beta / (\kappa \nu)$, $R_q = g\alpha h^6 \gamma / (\kappa^2 \nu)$,

$$\frac{\partial T}{\partial t} + (R_a - R_q \hat{z}^2)W = \nabla^2 T + Q, \quad (\text{A.7})$$

$$\frac{\partial Q}{\partial t} + R_q W = 0. \quad (\text{A.8})$$

Combining eqs. (A.6), (A.7) and (A.8) yields

$$\frac{\partial}{\partial t} \left[\left(\frac{\partial}{\partial t} - \nabla^2 \right) \left(\sigma^{-1} \frac{\partial}{\partial t} - \nabla^2 \right) \nabla^2 + (R_q \hat{z}^2 - R_a) \nabla_1^2 \right] W + R_q \nabla_1^2 W = 0, \quad (\text{A.9})$$

where W is the vertical velocity. The behavior in the limit of vanishing γ (the term in the square brackets) is the familiar Rayleigh-Bénard stability problem which can be easily solved for the frictionless isothermal boundary conditions

$$W = \nabla^2 W = \nabla^4 W = 0 \text{ at } z = \pm \frac{1}{2},$$

with zero growth solutions

$$W = \sin \pi z \exp(i\mathbf{k} \cdot \mathbf{x})$$

at $R_a = R_{ac} = \frac{27}{4} \pi^4$,
and

$$\mathbf{k} \cdot \mathbf{k} = \frac{1}{2} \pi^2$$

where \mathbf{k} is a two-vector in the (x, y) plane. Inspection of eq. (A.9) shows that a nonoscillatory zero growth solution is impossible for finite R_q unless $W = 0$. We therefore search for zero growth oscillations.

For small R_q , let

$$W = \exp(pt) \sin \pi z \exp\{i(\mathbf{k} + \mathbf{h}) \cdot \mathbf{x}\},$$

and the operator ∇^2 becomes

$$\frac{1}{2} \pi^2 + 2(\mathbf{k} \cdot \mathbf{h})^2 + h^2.$$

It is to be expected that \mathbf{h} and p will be some function of $(R_q)^n$ where $n > 0$, so that it vanishes as $R_q \rightarrow 0$. Therefore, for small R_q , only the lowest powers of p , \mathbf{h} and R_q are retained. Substituting into eq. (A.9) then yields

$$\frac{9}{4} \pi^2 (\sigma^{-1} + 1) p^2 + 24 \pi^2 (\mathbf{k} \cdot \mathbf{h})^2 p + \pi^2 R_q = 0, \quad (\text{A.10})$$

whose solution is

$$p = \left[-24 \pi^2 (\mathbf{k} \cdot \mathbf{h})^2 \pm \sqrt{24^2 \pi^4 (\mathbf{k} \cdot \mathbf{h})^4 - 9 \pi^2 (\sigma^{-1} + 1) \cdot \pi^2 R_q} \right] \times \left[\frac{9}{2} \pi^2 (\sigma^{-1} + 1) \right]^{-1} \quad (\text{A.11})$$

Note that $p = p_r + ip_i$, with $p_r \leq 0$; and $p_i = 0$ when $(\mathbf{k} \cdot \mathbf{h})^2 = 0$, which defines the maximum growth rate, in which case the original neutral motions oscillate with frequency

$$p_i = \sqrt{\frac{24}{9\pi^2} \frac{R_q}{1 + \sigma^{-1}}}.$$

The dimensional period is

$$t = 3\pi^2 \frac{h^2}{\kappa} \sqrt{\frac{1+\sigma}{\sigma} \frac{\nu\kappa^2}{g\alpha\gamma h^6}},$$

which, for $\sigma \rightarrow \infty$

$$t = 3\pi^2 \sqrt{\frac{\nu}{g\alpha\gamma h^2}},$$

which is the same as in the previous example, eq. (3.6), for $\omega^2 \gg \lambda$, except for the constant in front. In pursuing this analysis to finite amplitude one finds that severe problems are encountered if $R_a - R_{ac} > R_q$. Physically, the cells overturn one cycle and destroy the gradient of the heat producing material and there is no way for this gradient to be restored. However, if $R_q > R_a - R_{ac}$, the oscillations merely grow to a finite state and persist as oscillating finite amplitude motion.

Acknowledgments

The author would like to acknowledge informative discussions with D. Griggs, W. V. R. Malkus and F. H.

Busse concerning various aspects of this work. Many of the tanks and floats used here, and in earlier unreported prototypes, were skillfully made by the late Paul Cox.

References

- ALLEN, C. W. (1964), *Astrophysical quantities*, 2nd ed. (Althone Press, London).
- ELDER, J. (1968), *Science Progr.* **56**, 1-33.
- HOWARD, L. N., W. V. R. MALKUS and J. A. WHITEHEAD (1970), (HMW), *Geophys. Fluid Dyn.* **1** 123-142.
- KRISHNAMURTI, R. (1970a), *J. Fluid Mech.* **42**, 295-308.
- KRISHNAMURTI, R. (1970b), *J. Fluid Mech.* **42** 309-320.
- LACHENBRUCH, A. H. (1968), *J. Geophys. Res.* **73** (22), 6977-6989.
- LE PICHON, X. (1968), *J. Geophys. Res.* **73** 3661.
- MAXWELL, A. E., R. D. VON HERZEN, K. J. HSU, J. E. ANDREWS, T. SAITO, S. F. PERCIVAL, JR., E. D. MILOW and R. E. BOYCE (1970), *Science* **168**, 1047-1059.
- MCCONNELL, R. K. (1968). In: R. A. PHINNEY, ed., *History of the Earth's crust* (Princeton Univ. Press, Princeton, N. J.).
- NEWELL, A. C. and J. A. WHITEHEAD (1969), *J. Fluid Mech.* **38** 279-303.
- OLIVER, J. and B. ISACKS (1967), *J. Geophys. Res.* **72** 4259-4275.
- ROBINSON, J. L. (1967), *J. Fluid Mech.* **30** 579-600.
- SEGEL, L. A. (1969), *J. Fluid Mech.* **38** 203-224.
- WHITEHEAD, J. A. (1971), *Am. Scientist* **59** 444-451.